Four-Wave Mixing in Nonlinear Fiber with Two Intracavity Frequency-Shifted Laser Pumps

Katarzyna Krupa, Michela Bettenzana, Alessandro Tonello, Daniele Modotto, Gabriele Manili, Vincent Couderc, Philippe Di Bin, Stefan Wabnitz, and Alain Barthélémy

***Abstract*— We experimentally study Bragg-type four-wave mixing frequency conversion in highly nonlinear fibers by using two independent frequency-shifted-feedback lasers. We obtain frequency conversion with partial coherent pumps when both lasers operate in the continuous-wave regime. Our experimental results compare well with numerical simulations, which take into account partial coherence of the two pumps.**

***Index Terms*— Fibers, four-wave mixing (FWM), frequency conversion, nonlinear optics, parametric processes.**

I. Introduction

FOUR-WAVE mixing (FWM) in fibers finds many applications in domains ranging from metrology [1] to all-optical ultrafast frequency conversion and signal processing [2]. Nonlinear effects in fibers with partially coherent pumps have recently attracted a great interest, in view of their potential for polarization-insensitive wavelength conversion and for their increased resilience to Stimulated Brillouin Scattering [3]. In this letter we focus our attention on a specific type of FWM, which is generally called wavelength exchange or *Bragg-Scattering* (BS-FWM). This kind of FWM has an intrinsic low-noise nature [4], which makes it potentially applicable for light-by-light manipulation even for very faint signals such as quantum keys [5], [6]. In our work we used a pair of partially coherent pumps.

In practical implementations with highly nonlinear fibers (HNLF), intense narrowband lasers cannot be used in view of the low threshold value of Stimulated Brillouin Scattering. One of the most common solutions to overcome this problem is the use of *ad-hoc* GHz-rate phase modulation driven by a pseudo-random bit-sequence generator [5]. Such a phase modulation can broaden the pump spectra while maintaining the idler and signal bandwidths. Quite strikingly, in our work we observed significant BS-FWM by using partially coherent and independent pumps. We compare here our experimental results with numerical simulations. Incidentally, we may notice that the use of partially coherent pumps provides a relatively low-cost solution for implementing BS-FWM. Instead of spectrum-sliced amplified spontaneous emission (ASE) [3], in our experiment we used two independent intracavity frequency-shifted feedback lasers (IFSL). The partial coherence of IFSL has been widely studied in metrology applications and in the field of astronomy, as star emulator. The amplified IFSL has been applied to enhance the Brillouin threshold in supercontinuum generation [7].

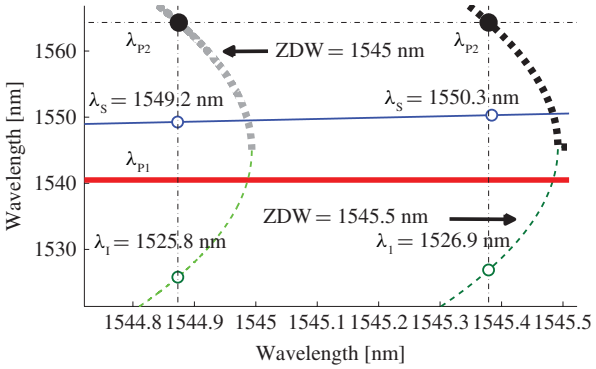

Fig. 1. BS-FWM phase-matching curves for two different ZDWs: thick solid (dashed) line (curve) for pump 1 (pump 2), thin solid (dashed) line (curve) for signal (idler).

II. Theory

Let us now briefly review the main properties of BS-FWM in a simplified treatment involving monochromatic waves only. The angular frequencies ω and the wave-vectors k for the pumps (P1, P2), signal (S) and idler (I) satisfy the following energy and wave-vector conservation conditions $\omega_I = \omega_S + (\omega_{P1} - \omega_{P2})$ and $k_I = k_S + (k_{P1} - k_{P2})$. When the signal frequency grows larger, the corresponding idler frequency also increases by the same amount. We approximated the wavelength dependence of the dispersion coefficient as a linear function. In Fig. 1 we present the phase-matching diagram for the BS-FWM with a zero-dispersion wavelength (ZDW) of 1545 nm (left-hand side diagram) or 1545.5 nm (right-hand side diagram). The dispersion slope was of 0.018ps/(km·nm^2) in both cases. The horizontal axis provides a common reference wavelength: its angular frequency is the mean value between the frequency of the idler and that of pump 2. Following the procedure of [5] we fix the wavelength of

Manuscript received June 13, 2011; revised October 29, 2011; accepted November 7, 2011. Date of publication November 16, 2011; date of current version January 25, 2012. This work was supported in part by the Region Limousin and in part by the French National Research Agency under Grant ANR-08-JCJC-0122 PARADHOQS.

K. Krupa, A. Tonello, V. Couderc, P. Di Bin, and A. Barthélémy are with Université de Limoges, XLIM, Limoges 87060, France (e-mail: katarzyna.krupa@xlim.fr; alessandro.tonello@unilim.fr; vincent.couderc@xlim.fr; philippe.dibin@xlim.fr; alain.barthelemy@xlim.fr).

M. Bettenzana, D. Modotto, G. Manili, and S. Wabnitz are with Dipartimento di Ingegneria dell'Informazione, Università di Brescia, Brescia 25123, Italy (e-mail: miki_bett@hotmail.it; daniele.modotto@ing.unibs.it; gabriele.manili@ing.unibs.it; stefano.wabnitz@ing.unibs.it).

Color versions of one or more of the figures in this letter are available online at http://ieeexplore.ieee.org.

Digital Object Identifier 10.1109/LPT.2011.2176328

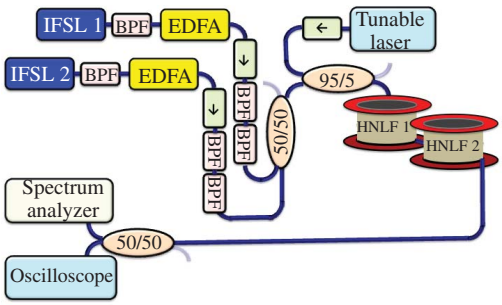

Fig. 2. Experimental setup.

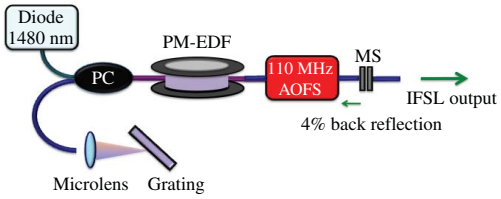

Fig. 3. Setup of IFSL. MS: Mating sleeve. PM-EDF: Polarization-maintaining erbium-doped fiber. PC: diode pump combiner.

pump 1 to 1540.5 nm. Let us focus first on the case of ZDW = 1545 nm. Taking into account our experimental constraints we fix the pump 2 to 1564.5 nm: from this wavelength we draw a vertical line that intersects both the thin solid line (signal wavelengths) and the thin dashed curve (corresponding idler wavelengths). The vertical coordinates of these crossings provide the optimal wavelengths for the signal (1549.2 nm, between the two pumps) and the corresponding idler (1525.8 nm, outside the two pumps). As shown in Fig. 1, for the same pump wavelengths (λ_{P1} and λ_{P2}) the optimal signal shifts to 1550.3 nm when ZDW = 1545.5 nm. In practice, the ZDW may fluctuate by about 1 nm along the fiber length, according to the analysis presented in [1] for similar types of fibers.

Our experimental setup is presented in Fig. 2. The two pumps are implemented by amplifying two independent IFSLs with distinct erbium doped fiber amplifiers (EDFAs).

III. Experimental Setup

To reduce the contribution of ASE, we placed 3 thin-film band-pass filters (BPF, 5 nm bandwidth): one of them before and two after each of the EDFAs. Optical isolators protect the EDFAs and IFSLs from back-reflections. The signal is provided by a commercial tunable narrowband extended cavity (ECL) laser with 4 mW output power. A 50/50 fiber coupler combined the two pumps, and a 95/5 "tap" coupler added the signal. Next, pumps and signal were injected in two cascaded off-the-shelf segments of HNLF: a 450 m long HNLF1 with the nominal ZDW of 1545 nm, and a 350 m long HNLF2 with the ZDW of 1546 nm. The output spectrum was observed by an optical spectrum analyzer or by a photodiode and an oscilloscope. The average powers of pump 1, 2 and signal as measured at the input of HNLF1 were 51.5 mW, 73.0 mW and 0.13 mW, respectively. In Fig. 3 we detail the structure of each IFSL. Each laser cavity is composed by a 20 m long polarization maintaining (PM) erbium doped fiber pumped by a laser diode emitting at 1480 nm. An intracavity acousto-optic frequency shifter (AOFS) was driven with a 110 MHz radio frequency generator. The IFSL cavity was bounded on one end by a fiber optic mating sleeve and on the other end by a microlens (4mm of focal length) and a blazed grating (600 groves/mm) in Littrow configuration. The free-space optics section is a key element for partial coherence and may also provide the frequency dependent loss. Indeed the laser bandwidth is roughly inversely proportional to the focal length. We fixed the central wavelengths of the two lasers at 1540.5 nm and 1564.5nm so to obtain the sources for pumps P1 and P2 to be amplified.

We observed that our IFSLs might operate in continuous wave (CW) or in a pulsed regime (see also [8]). In order to keep the IFSL lasers operating in the CW regime, we set the current of both laser pump diodes to 85 mA. For higher currents we observed a bifurcation into a time-periodic solution as outlined in Ref.[8]. The absence of relaxation oscillations was carefully monitored at the output of the IFSLs by using a 1 GHz photodiode connected to an oscilloscope.

IV. Comparison Between Numerical and Experimental Results

A key support for interpreting our measurements is provided by numerical solutions of the nonlinear Schrödinger equation (NLSE) involving two broadband pumps. In our simulations we employed the so-called phase diffusion model (PDM), which provides a Lorentzian shaped spectrum [9], [10]. Note that the PDM does not correspond to a rigorous description of the cyclostationary spectral properties of IFSLs [11]. In fact, we used the PDM as a validating tool for simulating broadband pumps with constant power in time domain with the aim of showing that BS-FWM is still visible with broadband pumps. In order to fit the experimental data, we combined the PDM with a numerical Gaussian filter. We experimentally measured the IFSLs bandwidth with the best available resolution of 6.2 GHz of our optical spectrum analyzer. Our experimental results give a 3 dB bandwidths of 36 GHz and 50 GHz for IFSL 1 and 2 respectively. The corresponding idler is 82.5 GHz wide at 1526.4 nm. In order to avoid numerical problems at the computation boundaries, each phase diffused pump was gated in the time domain by a 350 ps Gaussian pulse. In our numerical simulations we have used a 3dB bandwidth of 20 GHz and 30 GHz for pump 1 and 2 respectively. Since the experimental spectra of pumps and idler tend to zero much faster than the trend of a Lorentzian statistics, we have filtered the PDM output results with a 4^{th} order 100 GHz Gaussian filter. The resulting idler bandwidth is of 43.75 GHz at 1550 nm. We assumed a temporal peak power of 60 mW and 80 mW for pump 1 and 2 respectively. In Fig. 4 we compare the experimental output spectrum (top inset) with the average power spectrum obtained by repeatedly solving 50 times the NLSE. We consider first the case of two pumps only: here the lateral sidebands are induced by the standard nondegenerate FWM. Let us compare next experimental and numerical results of BS-FWM. To induce such type of FWM process we need a third tunable signal (between 1547 nm and 1554 nm).

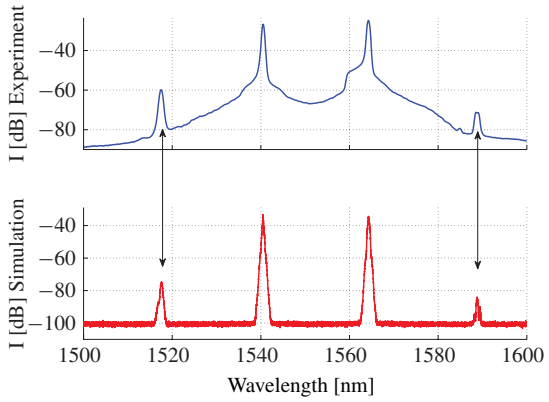

Fig. 4. Top: experimental result of output spectrum showing two pumps and two sidebands of nondegenerate spontaneous FWM. Bottom: corresponding numerical simulation.

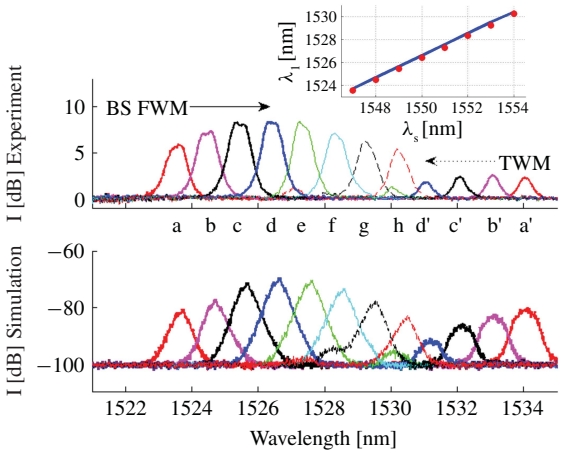

Fig. 5. Details of output spectra for idler of BS-FWM (a–h) and TWM (a'–d') for the signal wavelengths: 1547 nm (a, a'), 1548 nm (b, b'), 1549 nm (c, c'), 1550 nm (d, d'), 1551 nm (e), 1552 nm (f), 1553 nm (g), 1554 nm (h). Inset: numerical (blue line) and experimental (red dots) wavelength of BS-FWM idler versus signal wavelength.

Note from Fig. 4 the considerable wavelength-dependent noise background in the spectral region between 1520 nm and 1535 nm (due to the residual ASE noise from the EDFAs and the IFSLs), precisely where the BS-FWM idler is expected (see Fig. 1). This noise can be in principle reduced by stronger filtering. Here to discern our FWM conversion measurements from the ASE noise background, we display in Fig. 5 the ratio between the spectral intensities in the presence and in the absence of the input seed signal, respectively. In the top inset of Fig. 5 we show a series of measurements for various choices of signal wavelengths ranging from 1547 nm up to 1554 nm. The solid arrow indicates the wavelength up-shift (from position a to h) of the BS-FWM idler as the signal wavelength grows larger. These results confirm that the BS-FWM idler frequency is the sum of the signal frequency plus the beating between the two pump frequencies (which are fixed here). At maximum signal-to-idler conversion, we obtained a peak idler power 8 dB higher than the noise background. This value was 5 dB after the HNLF1. As confirmed by our simulations (not shown here), such low conversion efficiency is mainly due to the positions of the ZDW in the HNLFs as well as the pump wavelength spacing, which enhances competing FWM effects. Note also that, differently from setups involving *ad-hoc* phase modulation of the pumps, in our experiments the idler is also broadband. Fig. 5 also shows that another idler sideband is generated by three-wave mixing (TWM) from the signal around pump 1. As shown by positions a' to d', the second idler down-shifts as the signal wavelength grows larger. The corresponding numerical simulations have been calculated over an ensemble of 50 runs and the average spectral densities are shown on the bottom plot in Fig. 5. We modeled the signal as a narrowband 350 ps Gaussian pulse. Experiments and numerical simulations exhibit an excellent agreement and both show that the idler broadens as a result of the nonlinear interplay between the broadband pumps and the narrowband signal [6]. The inset of Fig. 5 presents the numerical (blue line) and experimental (red dots) wavelength dependence of idler upon signal: they grow larger just as it is expected in BS-FWM. In parametric phase conjugation instead, if the signal increases in wavelength the idler necessarily decreases its wavelength [5], [6].

V. Conclusion

In conclusion, we presented a detailed investigation of BS-FWM-based frequency conversion in a HNLF based on a pair of IFSL pumps. Although the conversion efficiency is relatively low in these experiments, the use of IFSLs may open new kind of applications in fiber nonlinear optics, such as the study and the rapid prototyping of all-optical frequency converters with reasonable budgets.

References

[1] B. Auguié, A. Mussot, A. Boucon, E. Lantz, and T. Sylvestre, "Ultralow chromatic dispersion measurement of optical fibers with a tunable fiber laser," *IEEE Photon. Technol. Lett.*, vol. 18, no. 17, pp. 1825–1827, Sep. 1, 2006.

[2] R. Slavík, *et al.*, "All-optical phase and amplitude regenerator for next-generation telecommunications systems," *Nature Photon.*, vol. 4, pp. 690–695, Sep. 2010.

[3] Y. Yan and C. Yang, "Four-wave mixing between coherent signal and incoherent pump light in nonlinear fiber," *J. Lightw. Technol.*, vol. 27, no. 22, pp. 4954–4959, Nov. 15, 2009.

[4] M. E. Marhic, Y. Park, F. S. Yang, and L. G. Kazovsky, "Widely tunable spectrum translation and wavelength exchange by four-wave mixing in optical fibers," *Opt. Lett.*, vol. 21, no. 23, pp. 1906–1908, 1996.

[5] A. H. Gnauck, R. M. Jopson, C. J. McKinstrie, J. C. Centanni, and S. Radic, "Demonstration of low-noise frequency conversion by Bragg scattering in a fiber," *Opt. Express*, vol. 14, no. 20, pp. 8989–8994, 2006.

[6] H. J. McGuinness, M. G. Raymer, C. J. McKinstrie, and S. Radic, "Quantum frequency translation of single-photon states in a photonic crystal fiber," *Phys. Rev. Lett.*, vol. 105, no. 9, pp. 093604-1–093604-4, 2010.

[7] P. A. Champert, V. Couderc, and A. Barthélémy, "1.5–2.0-μm multiwatt continuum generation in dispersion-shifted fiber by use of high-power continuous-wave fiber source," *IEEE Photon. Technol. Lett.*, vol. 16, no. 11, pp. 2445–2447, Nov. 2004.

[8] M. Stellpflug, G. Bonnet, B. W. Shore, and K. Bergmann, "Dynamics of frequency shifted feedback lasers: Simulation studies," *Opt. Express*, vol. 11, no. 17, pp. 2060–2080, 2003.

[9] A. Mussot, E. Lantz, H. Maillotte, T. Sylvestre, C. Finot, and S. Pitois, "Spectral broadening of a partially coherent CW laser beam in single-mode optical fibers," *Opt. Express*, vol. 12, no. 13, pp. 2838–2843, 2004.

[10] J. W. Goodman, "Statistical optics," in *Wiley Classics Library*. New York: Wiley, 1985.

[11] L. P. Yatsenko, B. W. Shore, and K. Bergmann, "Coherence in the output spectrum of frequency shifted feedback lasers," *Opt. Commun.*, vol. 282, no. 2, pp. 300–309, Jan. 2009.